Polar observations of transverse magnetic pulsations initiated at substorm onset in the high-latitude plasma sheet

P. K. Toivanen,[1,2] D. N. Baker,[1] W. K. Peterson,[1] H. J. Singer,[3] J. Watermann,[4] J. R. Wygant,[5] C. T. Russell,[6] and C. A. Kletzing[7]

Received 23 October 2001; revised 17 September 2002; accepted 20 February 2003; published 1 July 2003.

[1] This paper presents simultaneous observations of 6-mHz magnetic pulsations in the nightside high-latitude plasma sheet, inner plasma sheet at the geosynchronous distance, and auroral region on the ground in association with substorm onset. We study an isolated substorm ($AE \sim 300$ nT) onset on 19 October 1999 at ~0145 UT. The Polar spacecraft was located in the plasma sheet near the plasma sheet boundary and was magnetically conjugate with the Greenland west coast magnetometer chain. Polar measured large-amplitude transverse magnetic (10 nT; toroidal) and electric (20 mV m^{-1}) field oscillations (~6 mHz) during the early development of the negative bay (300 nT) in Greenland. On the ground, pulsations (50 nT) with the same frequency were superimposed on the negative bay. The geostationary GOES 8 spacecraft was located 2 hours west of Greenland. It observed compressional magnetic field oscillations (1 nT and ~6 mHz). At Polar the pulsations were initiated ~3 min before the first outward propagating substorm signature, an abrupt enhancement of the plasma sheet electron fluxes. Such a rich data set allows us to study in detail the spatial origin of the pulsations, their timing with respect to the negative bay onset, and their role in initiation of the substorm current wedge. It is concluded that the pulsations were initiated between the plasma sheet boundary and the tailward expanding region of the enhanced plasma sheet electron fluxes. The pulsations were then later observed on the ground and at GOES 8. It can also be argued that the pulsations were an integral part of the formation of the substorm current wedge. Finally, we suggest that the pulsations were generated by periodic variations in the rate of the current diversion from the braking region of the earthward flows generated by reconnection at the near-Earth neutral line. *INDEX TERMS:* 2788 Magnetospheric Physics: Storms and substorms; 2764 Magnetospheric Physics: Plasma sheet; 2740 Magnetospheric Physics: Magnetospheric configuration and dynamics; 2752 Magnetospheric Physics: MHD waves and instabilities; *KEYWORDS:* transverse pulsations, substorm onset signatures, onset timing, plasma sheet boundary, polar spacecraft

Citation: Toivanen, P. K., D. N. Baker, W. K. Peterson, H. J. Singer, J. Watermann, J. R. Wygant, C. T. Russell, and C. A. Kletzing, Polar observations of transverse magnetic pulsations initiated at substorm onset in the high-latitude plasma sheet, *J. Geophys. Res.*, *108*(A7), 1267, doi:10.1029/2001JA009141, 2003.

1. Introduction

[2] The substorm current wedge is a key element in the coupling between the geomagnetic tail and the ionosphere during magnetospheric substorms [*McPherron et al.*, 1973]. The current wedge is thought to be formed at substorm onset as a partial diversion of the cross-tail current into field-aligned currents that close through the ionosphere. The ionospheric part of the substorm current wedge forms the auroral electrojet, which is responsible for magnetic disturbances such as negative bays observed by ground-based magnetometers. Several mechanisms for the initiation of substorm current wedge have been assumed by substorm onset models such as the near-Earth neutral line (NENL) model [e.g., *Baker et al.*, 1996] and the current disruption model [e.g., *Lui*, 1996]. Thus observations of the formation of the substorm current wedge are important for understanding the physics of substorms and future development of the substorm models.

[3] Magnetic pulsations are a typical ground signature of substorm onset in a wide range of geomagnetic latitudes and longitudes. A class of these pulsations defined as Pi2 pulsations occurs in the period range from 40 to 150 s. These are closely correlated with other onset phenomena, including brightening of auroral arcs and electrojet intensi-

[1]Laboratory for Atmospheric and Space Physics, University of Colorado, Boulder, Colorado, USA.
[2]Now at Finnish Meteorological Institute, Helsinki, Finland.
[3]Space Environment Center, NOAA, Boulder, Colorado, USA.
[4]Danish Meteorological Institute, Copenhagen, Denmark.
[5]School of Physics and Astronomy, University of Minnesota, Minneapolis, Minnesota, USA.
[6]Institute of Geophysics and Planetary Physics, University of California at Los Angeles, California, USA.
[7]Department of Physics and Astronomy, University of Iowa, Iowa City, Iowa, USA.

0148-0227/03/2001JA009141$09.00

fications. Thus the Pi2 band has been used extensively in substorm studies, for example, to determine the onset time or location of the initial brightening. In space, according to statistical results of *Sakurai and McPherron* [1983], magnetic pulsations during substorm activity at geostationary distances can be classified primarily by two types of pulsations: (1) an irregular wave with a significant compressional component and (2) a pure quasi-sinusoidal transverse wave in the azimuthal component (toroidal). *Sakurai and McPherron* [1983] concluded that the pure transverse waves are quite rare, while the compressional wave occurs during almost every substorm. According to the statistical study by *Takahashi et al.* [1996] ~30% of the Pi2 events on the ground are accompanied by nightside transient toroidal pulsations in the frequency range of Pc3–Pc5.

[4] On the basis of theoretical considerations MHD transients are expected to be excited by any change in magnetopheric convection or configuration during substorms [*Southwood and Stuart*, 1980]. High-latitude and midlatitude Pi2 pulsations are thought to be caused by the sudden generation of field-aligned currents in association with the disruption of cross-tail currents in the plasma sheet [e.g., *Olson*, 1999]. Also, the flow channel of enhanced plasma flows generated by magnetic reconnection at the near-Earth neutral line is expected to excite Pi2 pulsations: the dawn-to-dusk electric field associated with the flow channel is propagated to the ionosphere as an Alfvén wave, and the field-aligned current associated with the wave initiates the substorm current wedge [e.g., *Baker et al.*, 1996]. Low-latitude Pi2s are thought to be a response of the inner magnetosphere to compressional waves generated at the substorm onset [e.g., *Olson*, 1999]. In contrast to the extensively studied Pi2 pulsations little attention has been paid to the transient toroidal pulsations and their generations mechanisms [*Takahashi et al.*, 1996. In general terms, these authors explained such pulsations as MHD transients produced by the reconfiguration of the near-Earth magnetotail. Considering the ambiguities in the generating mechanisms of the pulsations in the overlapping frequency ranges of Pi2s and Pc5s and the extensive use of this frequency range in the substorm studies, it is important to understand any processes generating pulsations in this frequency range to establish their role in substorm activity.

[5] An important way to consider the effects of various field variations in space on the substorm physics is the magnetic field-aligned Poynting flux associated with the variations. Recently, there have been several studies of large parallel Poynting flux on auroral magnetic field lines during substorm activity. *Toivanen et al.* [2001b] presented observations of large Poynting flux associated with magnetic field and plasma flow variations obtained by the Polar spacecraft in the high-latitude plasma sheet. Timing of these variations corresponded to the Pi2 and visible auroral onsets at magnetically conjugate ground stations [*Toivanen et al.*, 2001a]. Similar field variations occurring near or at the plasma sheet boundary during substorm activity have also been studied by *Keiling et al.* [2000]. According to *Wygant et al.* [2000], these variations and Poynting flux occur on auroral field lines conjugate to bright auroras as determined from the Ultra-Violet Imager (UVI) on board Polar. Parallel Poynting flux has also been reported by *Erickson et al.* [2000] in the CRRES spacecraft data sets. According to these authors, there is another source region of large parallel Poynting flux located in the near-Earth plasma sheet, and this region is associated with the near-geosynchronous onset mechanisms. As there seem to be two spatial sources of large parallel Poynting flux, it is important to present detailed multiplatform observations of electromagnetic field pulsations and associated Poynting flux in order to address the spatial origin, the timing with respect to various ground signatures, and the role of the pulsations in the initiation of the substorm current wedge and in the physics of substorms.

2. Observations

2.1. Ground Activity

[6] On 19 October 1999 an isolated substorm occurred with *AE* reaching ~300 nT. It was first observed shortly before 0145 UT by the southernmost of the Greenland magnetometers in Narsarsuaq (NAQ; 66.31 CGM latitude, 43.91 CGM longitude). Figure 1 shows the northward (Figure 1a), eastward (Figure 1b), and vertical (Figure 1c) components as functions of time at the Greenland west coast stations (Figure 2). The vertical line at 0144:23 UT marks the initiation of the substorm-related signatures at Polar as defined in section 2.5. The northward component shows a very weak deflection (~7 nT) at NAQ beginning at ~0142 UT, but the actual northward expansion of the negative deflections took place after 0145 UT. The latitude of the auroral electrojet can be identified as the boundary between positive and negative deflections of the vertical component (Figure 1c): At ~0147 UT, the electrojet was located at NAQ and was moving northward. The positive deflection from 0145 UT to 0147 UT at NAQ, FHB, and GHB implies that the electrojet enhancement initiated south of NAQ. Prior to 0145 UT, only a weak deflection of the vertical component can be identified, and no substorm electrojet existed before 0145 UT within or in the vicinity of the west coast chain. The key features of this event are the large-magnitude magnetic pulsations in a timescale of a few minutes starting shortly after 0145 UT, lasting until about 0205 UT, and following with the northward propagation of the auroral electrojet. These can be seen as periodic variations in all three components shown in Figure 1.

[7] It can also be argued that the auroral electrojet was meridionally favorably located with respect to the Greenland chain. After 0145 UT, the magnitude of the eastward deflection is small relative to the values observed after 0150 UT. The negative eastward component after 0150 UT may suggest that the magnetic chain was located between the downward and upward field-aligned currents of the current wedge. Midlatitude magnetometers located east and west of Greenland provide supplement observations in determination of the substorm electrojet location. East of the Greenland the magnetometers in Hella (HLL; 64.49 CGM latitude, 68.36 CGM longitude) and Faroes (FAR; 60.76 CGM latitude, 78.10 CGM longitude) of the SAMNET magnetometer chain observed a negative bay and sequence of the Pi2 pulsatations (~17 mHz), respectively, starting at about 0146:30 UT (Figure 3). Analysis of the SAMNET data using the model of *Cramoysan et al.* [1995] shows that the downward FAC of the current wedge was located west

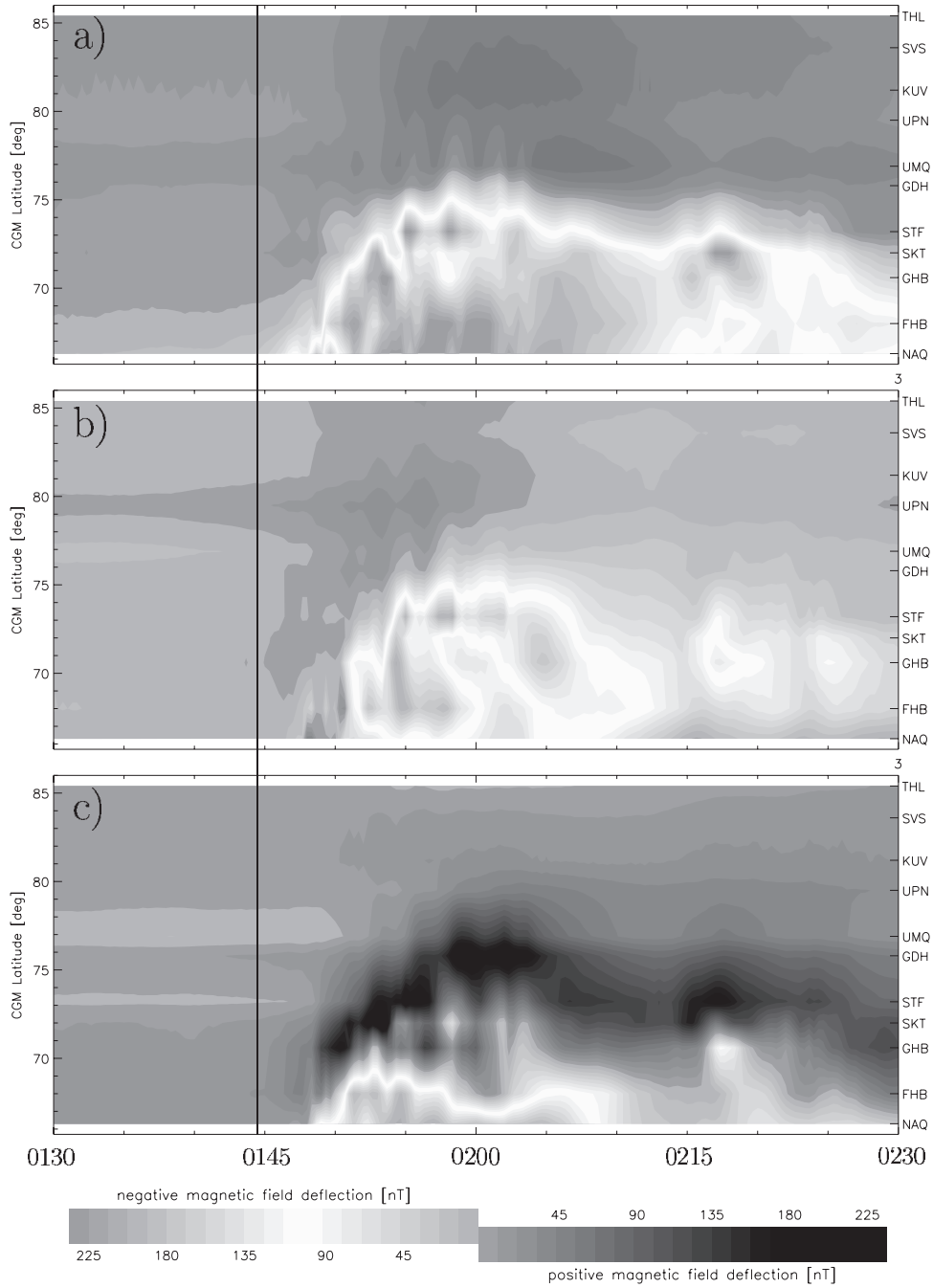

Figure 1. Deflections of the horizontal (a) north-south and (b) east-west, and (c) vertical magnetic field CGM components as functions of CGM latitude and time (CGM, Corrected Geomagnetic). The magnitudes were interpolated in the latitude range of the Greenland west coast stations. At 0144:23 (vertical line), Polar observed the first dynamical signatures (defined in Figure 8k) associated with the ground onset. See color version of this figure at back of this issue.

of SAMNET (D. K. Milling, private communication 2002). Figure 4 shows midlatitude magnetic field perturbations west of Greenland in Ottawa (OTT; 56.7 CGM latitude, 0.1 CGM longitude) and St. John's (STJ; 54.6 CGM latitude, 13.2 CGM longitude). During the early expansion phase, the positive deviation of the Y component at STJ (and OTT) suggests that the center of the substorm current wedge was located east of STJ. On the other hand, the positive X component at STJ indicates that the center of the upward FAC current was located west of STJ. The small deviations of the X component from the baseline at OTT indicate that OTT was located near the reversal of the positive and negative deviations of X associated with the upward FAC of the substorm current wedge. The positive deviations of the X component after ~0200 UT at OTT, can then be considered as a signature of the approach of the upward FAC to OTT. On the basis of these available observations and the interpretations made, it can be concluded that the current

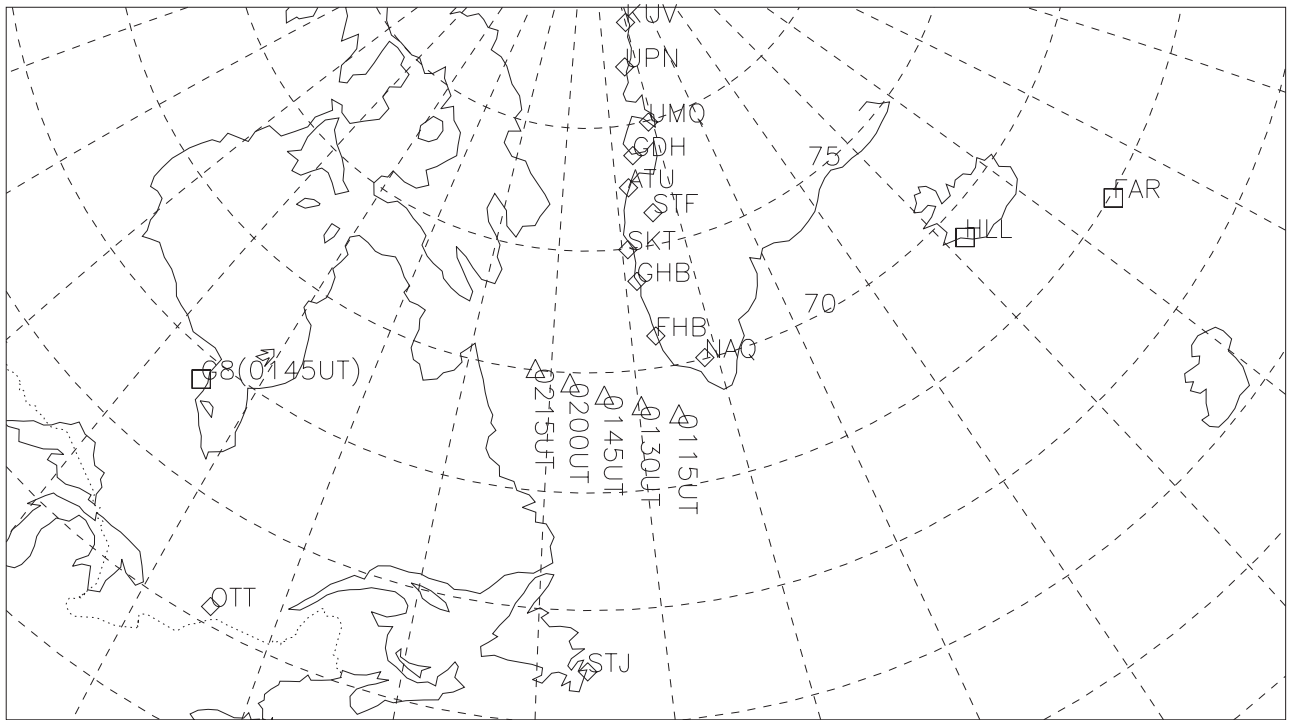

Figure 2. The ionospheric foot points of Polar from 0115 to 0215 UT (triangles) and GOES 8 at 0145 UT (squares) as determined from the T89 and IGRF models. The Greenland west coast magnetometers, south of Kullorsuaq (KUV), are indicated with diamonds. The two westernmost stations of SAMNET in Hella (HLL) and Faroes (FAR) are indicated with squares. The dashed lines are the geomagnetic latitudes and longitudes.

wedge was initiated preferably with respect to the Greenland sector.

2.2. Solar Wind Conditions

[8] The Geotail and IMP8 spacecraft were located in the upstream solar wind at $\mathbf{r}_{GSM}$ = (6, −26, 5) R_E and $\mathbf{r}_{GSM}$ = (18, −33, 15) R_E, respectively. Both spacecraft observed steady solar wind conditions during the event starting at 0125 UT after a reduction of the $B_{Z_{GSM}}$ component of the interplanetary magnetic field from −2 nT to zero.

2.3. Locations of the Polar and GOES 8 Spacecraft

[9] Figure 5 shows the locations of the Polar and GOES 8 spacecraft in the noon-midnight meridian (Figure 5a) and the magnetic field line locations of these spacecraft and selected ground stations in the equatorial current sheet (Figure 5b). A superposititon of the International Geomagnetic Reference Field (IGRF) and the magnetic field model of *Tsyganenko* [1989] (T89) was used to determine the locations of the field lines in the equatorial current sheet. In addition to the dipole tilt angle, the T89 model requires the *Kp* index as input. It was determined by comparing the actual Polar magnetic field measurements obtained by the Magnetic Field Experiment (MFE) [*Russell et al.*, 1995] with the T89 model predictions. The best fit to the data was achieved by using *Kp* = 2. At 0145 UT, the Polar and GOES 8 spacecraft were located in the premidnight sector at $\mathbf{r}_{GSM}$ = (−6.6, 1.0, 0.7) R_E and $\mathbf{r}_{GSM}$ = (−4.4, 4.9, −0.3) R_E, respectively. Since the dipole tilt angle during this event was approximately −17°, these spacecraft were not located as close to the magnetic equator as their Z_{GSM} coordinates may indicate. According to Figure 5a, it is apparent, that the spacecraft separation of ∼1 R_E in Z_{GSM} leads to a considerable separation in the equatorial current sheet. At 0145 UT, the magnetic field lines of Polar and GOES 8 mapped to $\mathbf{r}_{GSM}$ = (−15.1, 2.5, −2.4) R_E and $\mathbf{r}_{GSM}$ = (−4.4, 5.2, −1.0) R_E (Figure 5b). The locations of the field lines of NAQ, HLL, and FAR at 0145 UT are also shown.

[10] In addition to the magnetic field mapping, direct information of the Polar location in the tail can be obtained from actual Polar measurements. Figure 6 shows an over-

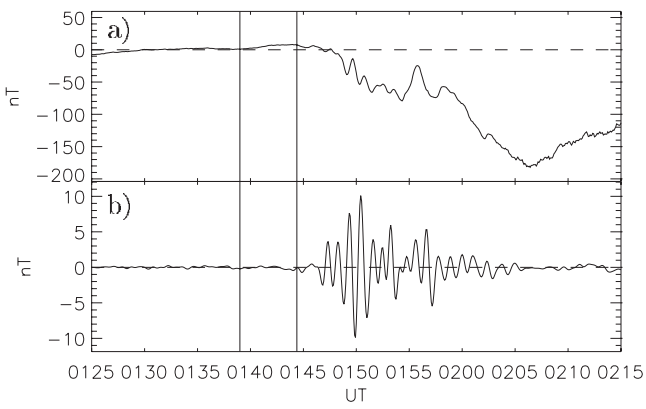

Figure 3. (a) Deflection of the magnetic field (geomagnetic northward component; top panel) at HLL of SAMNET. (b) Pi2 pulsations at FAR (geomagnetic northward component filtered; bottom panel).

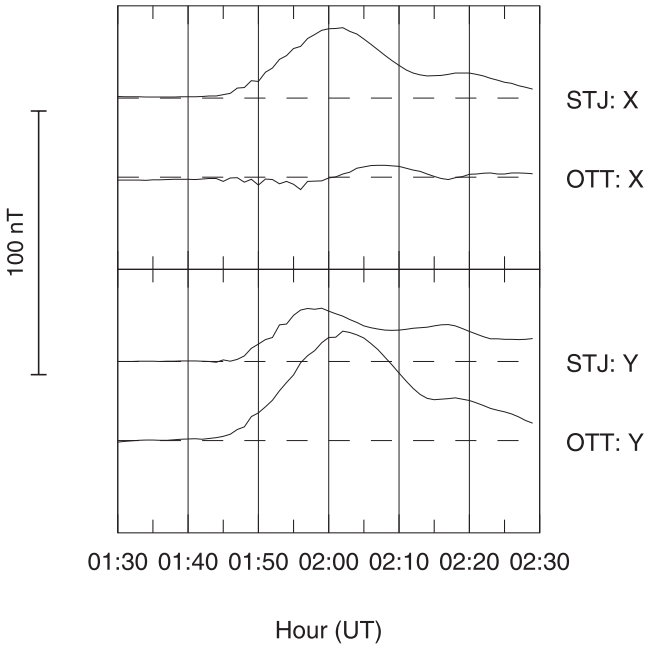

Figure 4. Midlatitude magnetic field X and Y component in Ottawa (OTT) and St. John's (STJ).

view of selected Polar measurements during the event (outward pass from the outer electron radiation belt to the tail lobe). Figure 6a shows high-energy electron fluxes as measured by the Imaging Electron Sensor of Comprehensive Energetic Particle and Pitch Angle Distribution Experiment [*Blake et al.*, 1995] (CEPPAD\IES). The outer electron belt can be associated with the high fluxes before ~0130 UT (the enhanced fluxes after ~0145 UT are related to the substorm activity). The plasma sheet electron population was observed by the HYDRA instrument [*Scudder et al.*, 1995] (Figure 6b). The sharp decrease of the electron fluxes at ~0237 UT indicates the boundary between the plasma sheet and the northern tail lobe. Prior to the boundary crossing, the Polar spacecraft potential measured by the Electric Field Instrument (EFI) [*Harvey et al.*, 1995] dropped suddenly in response to low electron fluxes in the vicinity of the plasma sheet boundary. Comparison of the electron fluxes and the spacecraft potential observed at ~0145 UT to those observed near the plasma sheet boundary at 0237 UT, suggests that Polar was located near the plasma sheet boundary at ~0145 UT.

[11] In the ionosphere, the foot point of Polar at 0145 UT was located ~1.4° south and ~10° west of NAQ and ~40° east of the foot point of GOES 8 (Figure 2). As the auroral electrojet enhancement initiated south of NAQ and near the Greenland west coast, the Polar foot point was favorably located with respect to the early changes in the electrojet.

2.4. Magnetic Field Observations at GOES 8

[12] Figures 7a–7c show magnetic field measurements in a magnetic field-aligned coordinate system at GOES 8: X is aligned with the ambient field (the observed field boxcar-averaged with width of 35 min); Y is perpendicular to the plane defined by the X component and the radius vector to the spacecraft position (positive toward the west); and Z completes a right-handed triad. Figure 7d shows the elevation angle of the magnetic field at GOES 8. In order to best represent temporal variations of the magnetic field elevation, a linear trend has been substracted from the elevation angle defined as 180 $\arctan(B_H/B_V)/\pi$, where B_H and B_V are the magnetic northward and radial components, respectively. Such a linear trend is introduced by the motion of GOES 8 toward the nightside as deduced from the T89 model in the given timescale of an hour. From 0145 to 0155 UT, the magnetic field was fairly constant relative to the deflections observed after 0155 UT (the periodic fluctuations during 0145–0155 UT are studied in detail in sections 2.5 and 3). The negative (0155–0207 UT) and then positive (after 0207 UT) deflections can be interpreted as a passage of the upward field-aligned current of the substorm current wedge tailward of GOES 8. This is most probably related to the westward expansion of the current wedge observed at OTT.

2.5. Polar Observations

[13] Figure 8 shows observations of several instruments onboard Polar in comparison with the observations of GOES 8 and NAQ summarized in Figures 8a, 8b, and 8c. The X (posititive magnetic north) component of the magnetic field variations at NAQ indicates the earliest signature of the negative bay onset at ~0145 UT (Figure 8a). In order to study the pulsations superimposed on the developing electrojet, Figure 8b shows the X component at NAQ after detrending over 180 s. The detrending was carried out by boxcar-averaging the original signal with a width of 180 s and subtracting the average signal from the original signal. The amplitudes of the pulsations ~50 nT were considerable in comparison with the magnitude of the negative bay (~300 nT; Figure 8a). At GOES 8, magnetic pulsations with amplitudes of the order of 1 nT were observed in close temporal association with the ground pulsations (Figure 8c; the ambient field at GOES 8 shown in Figure 7a detrended over 180 s). The electron data from the CEPPAD/IES and HYDRA instruments shown in Figures 6a and 6b are replotted in Figures 8d and 8e, respectively. Figures 8f, 8g, 8h, and 8i show magnetic field data obtained from the MFE instrument. The elevation angle of the magnetic field ($\alpha_{\mathrm{MFE}} = 180 \arctan(B_{Z_{\mathrm{GSM}}}/B_{X_{\mathrm{GSM}}})/\pi$) is shown in Figure 8f as $\delta\alpha_{elevation} = \alpha_{MFE} - \alpha_{T89}$, where α_{T89} is the elevation angle of the T89 model. Figures 8h and 11i show the magnetic field components B_Y and B_Z perpendicular to an ambient magnetic field at Polar. The ambient field (Figure 8g) was determined by boxcar-averaging (180 s) the total magnetic field measured by MFE. The coordinate system used (same as in Figure 7) is convenient during the interval since $(X, Y, Z) \approx (X_{GSM}, Y_{GSM}, Z_{GSM})$. Figures 8j and 8k show the electric field measurements obtained from EFI. Finally, Figure 8l shows the Poynting flux parallel to the ambient field (the positive values correspond to Poynting fluxes directed toward the ionosphere).

[14] The key features of the Polar field measurements are the prominent oscillations initiated both in close proximity to the negative bay onset and prior to the pulsations observed on the ground and at GOES 8 (spectral analysis of these pulsations is presented in section 3). The large parallel Poynting flux with a peak magnitude of ~0.5 ergs $\mathrm{cm}^{-2}\ \mathrm{s}^{-1}$ associated with these oscillations indirectly indicates that Polar was magnetically conjugate to bright

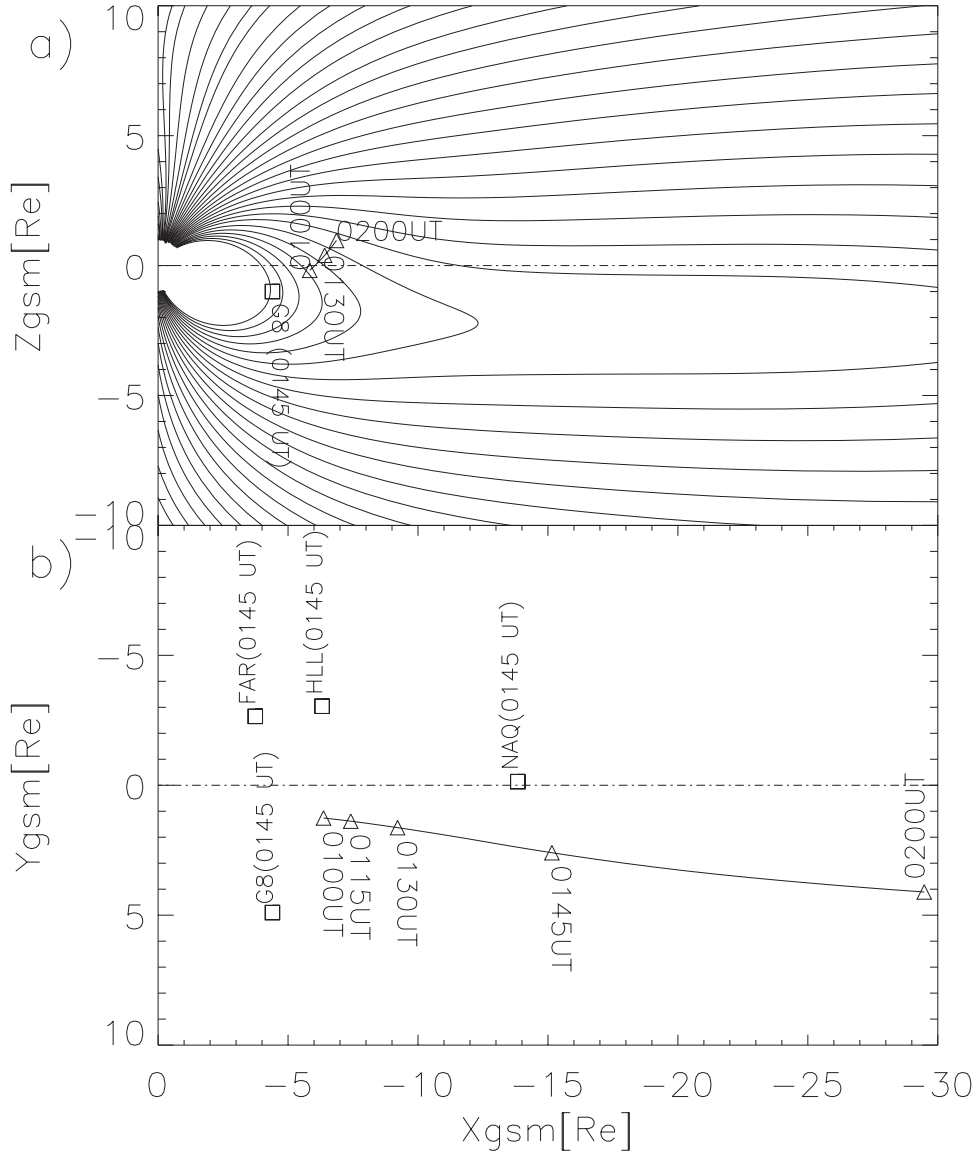

Figure 5. (a) Polar orbit during the event in the noon-midnight meridian. Note the relatively large dipole tilt angle because of which, at 0145 UT, (b) the Polar field line maps clearly further in the equatorial current sheet than that of GOES 8. The mappings of the field lines of the magnetic stations of NAQ (Narsarsuaq), HLL (Hella), and FAR (Faroes) at 0145 UT are indicated with a square. The magnetic field line mappings were made using a superposition of the T89 and IGRF models.

auroras. Considering the time of the oscillations and the large Poynting flux toward the ionosphere, we define the substorm onset time to be the first enhancement in the magnetic (~4 nT; Figure 8h) and electric fields (~10 mV m^{-1}; Figure 8k) at 0144:23 UT. The magnetic field configuration started to become more dipolar ~2 min after the onset time as indicated by the elevation angle in Figure 8f.

[15] The important aspect of the particle data is the abrupt increase of the electron flux at ~0147:30 UT as measured by HYDRA about 3 min after the onset (Figure 8e). Such increases are typically caused by plasma boundaries moving with respect to the spacecraft. At this time, one can also identify a sharp gradient in the ambient magnetic field (Figure 8g) presumably caused by the diamagnetic effect of the enhanced particle fluxes. Note also that the Poynting flux peaked at this boundary.

[16] Prior to the onset, there were weak dynamic signatures at Polar and GOES 8 at 0139:00 UT. On the ground, only a weak signature can be identified. Between 0139 and 0145 UT the decrease of the magnetic field X components both at Polar (Figure 8g) and at GOES 8 (Figure 7a), suggests that the signature was rather a causal precursor of the onset than a transient perturbation.

3. Spectral Analysis of the Observed Pulsations

[17] Further analysis of the pulsations observed at Polar, GOES 8, and on the ground is based on the Fast Fourier Transformation (FFT). The time interval transformed into the frequency domain ranges over an integer number of cycles with a period of 180 s. The period of 180 s was estimated from the time series shown in Figures 8b, 8c, and

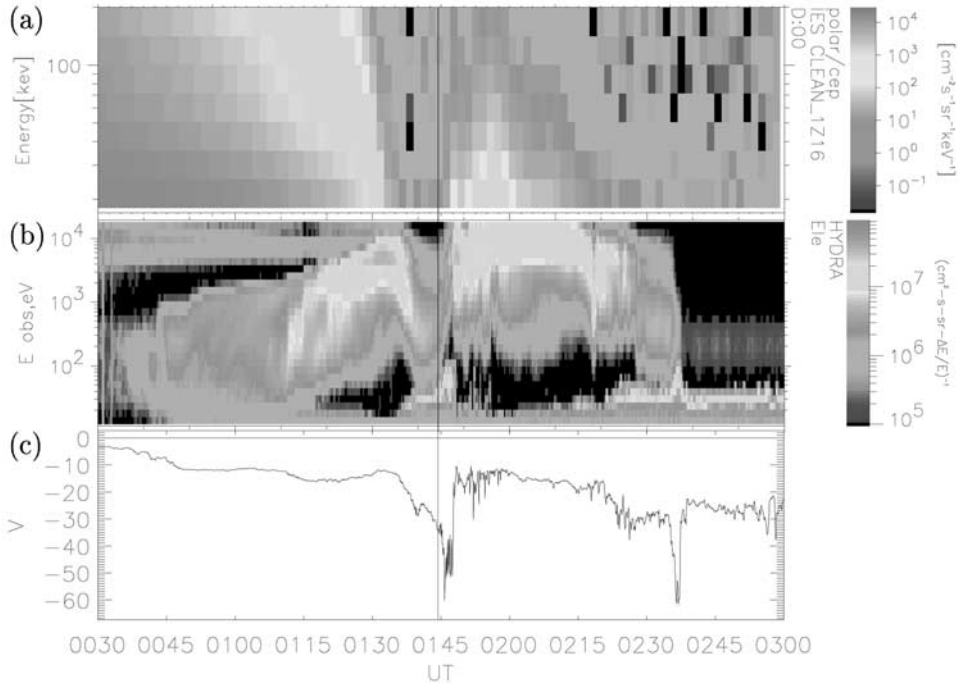

Figure 6. Overview of (a) high-energy electrons (17–200 keV), (b) plasma sheet electrons (0.1–20 keV), and (c) spacecraft potential as observed by CEPPAD/IES, HYDRA, and EFI, respectively. See color version of this figure at back of this issue.

8h. Such time intervals are used in order to reduce smearing of the frequency component of interest: substantial smearing can be expected as only a small number of cycles with period of ~180 s are present in the time series, especially in B_Y at Polar.

[18] At Polar, the pulsations occurred mostly in the B_Y component. This can be verified by the amplitude spectra of the signals of Figures 8g, 8h, and 8i (Figure 9). The spectra of the B_X and B_Z are relatively flat compared to the spectrum of the B_Y component. Its spectrum shows two peaks, one centered around 6.5 mHz (maximum amplitude at 5.6 mHz) and the other around 18 mHz. As the B_Y component is roughly aligned with Y_{GSM}, the pulsations can be considered as toroidal.

[19] At GOES 8, the compressional component (B_X) has an amplitude spectrum peaked in the same frequency range as the spectrum of the toroidal pulsations at Polar (Figure 10). The frequencies higher than 10 mHz are mainly caused by the transverse components (B_Y and B_Z). The amplitude of the compressional pulsations at GOES 8 is smaller by an order of magnetitude than that observed at Polar.

[20] In order to compare the spectra of the toroidal (B_Y) pulsations at Polar and the compressional pulsations at GOES 8 to the spectrum of the pulsations at NAQ, Figure 11 shows the spectrum of the detrended northward component at NAQ (dotted line). It is peaked in the same frequency range as B_Y at Polar and B_X at GOES 8. In addition, the spectrum of the electric field E_Z component at Polar is also shown with dash-dotted line. It has characteristics similar to those of the magnetic field B_Y component at Polar. This justifies the filtering of the electric field signals in Figures 8j and 8k.

[21] Finally, we study the phase shifts between the signals of Figures 8b (NAQ: detrended X_{NAQ}), 8c (GOES

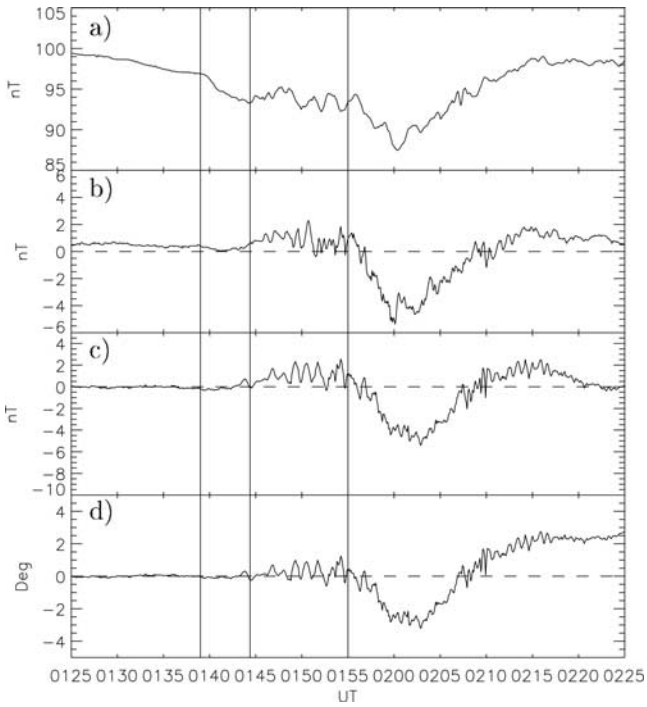

Figure 7. (a) The ambient magnetic field X and the components (b) Y and (c) Z, perpendicular to the ambient field at GOES 8 (see text for the definition of the coordinate system used). (d) Elevation angle of the magnetic field (see text for the definition). The vertical lines indicate a dynamic signature at Polar prior to the onset (0139:00 UT; deduced from Figure 8k), the onset time defined from the Polar observations (0144:23 UT; Figure 8k), and the beginning of a magnetic field variation perpendicular to the ambient field at GOES 8 (0155:00 UT).

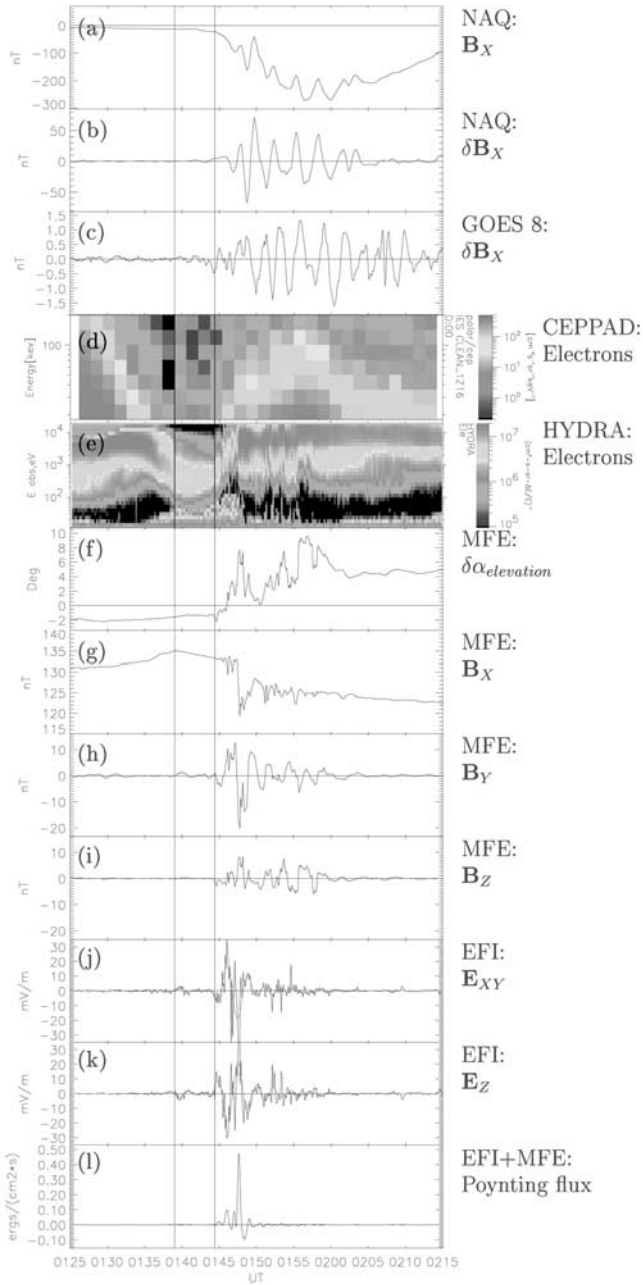

Figure 8. (a) The northward component at NAQ, (b) the 180-s detrended northward component at NAQ, (c) the 180-s detrended ambient field at GOES 8, (d) CEPPAD electrons (17–200 keV), (e) HYDRA electrons (0.1–20 keV), (f) measured magnetic field elevation angle with respect to the elevation angle of the T89 model, (g) ambient magnetic field at Polar, (h) Y and (i) Z components of the perpendicular magnetic field at Polar, (j) XY_{GSE} and (k) Z_{GSE} components at Polar (the red curves show the low-pass filtered (<7 mHz) 180-s detrended signals), and (l) Parallel Poynting flux (positive toward the ionosphere). The vertical lines indicate the onset time (0144:23 UT) and the transient signature at 0139:00 UT as determined from the EFI instrument (Figure 8k). See color version of this figure at back of this issue.

8: B_X), 8h (Polar: B_Y), and 8k (Polar: E_Z). First, the signals were low-pass filtered based on the spectral analysis shown in Figure 11. Figure 12 shows cross correlations as functions of lag time from the onset time. At Polar, B_Y and E_Z are anticorrelated with a phase shift of 33 s (lag time: 33 s), which can also be verified by comparing the time series of B_Y and E_Z in Figures 8h and 8k. The correlation coefficient is 0.88. The ground response (detrended X_{NAQ}) is delayed by 117 s with respect to B_Y at Polar (Figure 12; dotted line). In this case, the correlation coefficient is 0.63. The maximum correlation coefficient of B_Y at Polar and B_X at GOES 8 is only 0.37 with time lag of 105 s (Figure 12; dashed line), although the spectra of these two signals are very similar to each other. Since such a low correlation, the cross correlation between detrended X_{NAQ} and B_X at GOES 8 is also shown in Figure 12 (dash-dotted). The maximum correlation coefficient of these two signals is 0.68 with lag time of 129 s. This implies that B_X at GOES 8 was delayed by 246 s from B_Y at Polar. On the basis of these phase shifts, we conclude that the pulsations in the frequency range around 6 mHz at GOES 8 and on the ground at NAQ were delayed at least about 2 min from the pulsations observed at Polar.

4. Pulsations and Substorm Activity

[22] In order to interpret the presented observations, we seek answers to three questions: (1) How are the pulsations related to the auroral electrojet and substorm current wedge; (2) What is the spatial origin of the pulsations; and (3) What is the relation of the variations to the plasma sheet dynamics.

[23] The oscillations at Polar occurred in very close proximity to the negative bay onset. Note that the use of ground magnetometers may introduce an uncertainty in the timing of the initial auroral brightening. A time lag between the magnetograms and the auroral break up can be introduced, if the breakup did not occur in the meridian of the magnetometer chain. As there were no global auroral images, this cannot be fully confirmed. On the basis of the midlatitude magnetometer data, the center of the upward FAC of the current wedge was located east of OTT and west of STJ, and the center of the current wedge was located east of STJ during the early expansion phase. According to the observations of the SAMNET stations, the downward FAC of the current wedge was located west of the SAMNET stations. These observations indicate that the current wedge was initiated around the meridian of the Greenland west coast stations.

[24] Furthermore, indirect evidence of Polar being magnetically conjugate with the auroral break up area can also be presented. As mentioned earlier, the large parallel Poynting flux indicates strong auroral activity near the Polar ionospheric foot point since large Poynting fluxes on auroral field lines have been shown to be magnetically conjugate with bright auroral displays [*Wygant et al.*, 2000]. In addition, the amplitude of the magnetic oscillations (~50 nT) on the ground were a considerable fraction of the magnitude of the negative bay (~300 nT). The oscillations were closely related spatially to the auroral electrojet as they followed the poleward movement of the electrojet (Figure 1). These considerations suggest that the oscillations were an integral part of the initiation of the substorm current wedge and the substorm onset.

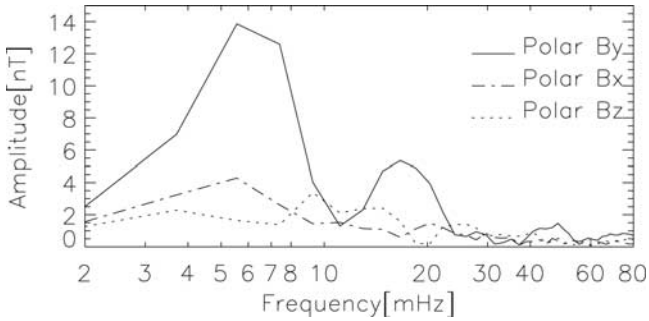

Figure 9. Amplitude spectra of the compressional (B_X; dash-dotted line) and transverse (B_Y and B_Z; solid and dotted lines, respectively) magnetic pulsations at Polar.

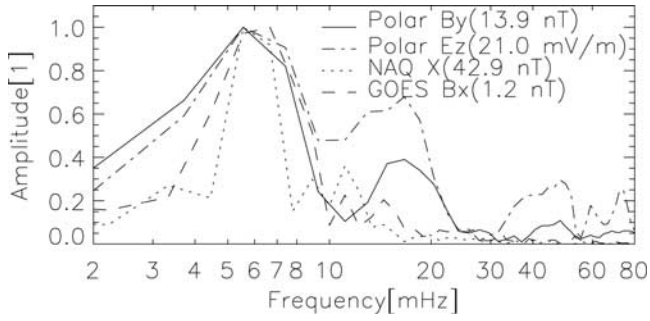

Figure 11. Amplitude spectra of the transverse B_Y component at Polar (solid line), electric field Z_{GSE} component at Polar (dash-dotted line), magnetic field northward component at NAQ (dotted), and compressional magnetic field compenent at GOES 8 (dashed). Each spectra is normalized to the maximum amplitude given in the upper corner of Figure 11.

[25] We argue that the oscillations were initiated near the plasma sheet boundary rather than in the inner magnetosphere. According to the magnetic field model used (T89), the Polar field line mapped to $X_{GSM} = -15.1\ R_E$. During the substorm growth phase, the magnetic field configuration is more stretched than that of T89 [*Pulkkinen et al.*, 1991], and mapping of the Polar field line even further in the tail might be expected. Such a mapping is supported by the HYDRA electron measurements, since, prior to the onset time, these measurements indicated that the plasma sheet was relatively thin at Polar, if compared to the extent of the plasma sheet after the substorm. The low electron flux observed by HYDRA indicate that Polar was located in the vicinity of the plasma sheet boundary. This conclusion is also consistent with the spacecraft potential measured by EFI. *Toivanen et al.* [2001b] noted a similar discrepancy in the location of the Polar field line in the nightside plasma sheet deduced from magnetic field mapping and from the particle measurements: according to the magnetic field mapping the Polar field line crossed the equatorial current sheet at $X_{GSM} \sim -10\ R_E$, whereas the particle measurements indicated that Polar was actually in the tail lobes. Furthermore, high-frequency electromagnetic oscillations and associated parallel Poynting fluxes similar to those in the event studied have typically been observed near or at the plasma sheet boundary during substorms [*Keiling et al.*, 2000]. These arguments suggest that the Polar field line mapped close to the distant X-line separating the tail lobes and plasma sheet.

[26] The magnetic field observations at GOES 8 are in accordance with the interpretation of the Polar data, the oscillations were not initiated in the inner magnetosphere. The amplitudes of the 6-mHz oscillations at Polar were larger by a factor of 10 than those observed at GOES 8. In principle, small amplitudes at GOES 8 could be explained if the node of the pulsations was located near GOES 8 at the magnetic equator. However, the exponential decay of the pulsations at Polar is more coherent than the waveform observed at GOES 8. Finally, the oscillations were first observed at Polar and only later at GOES 8. These arguments imply a radial propagation of these oscillations inward rather than outward. In addition, the elevation angle of the magnetic field at GOES 8 indicated that upward field-aligned current was located tailward of GOES 8. This indicates that the region of current disruption and the substorm current wedge were located outside the geostationary orbit.

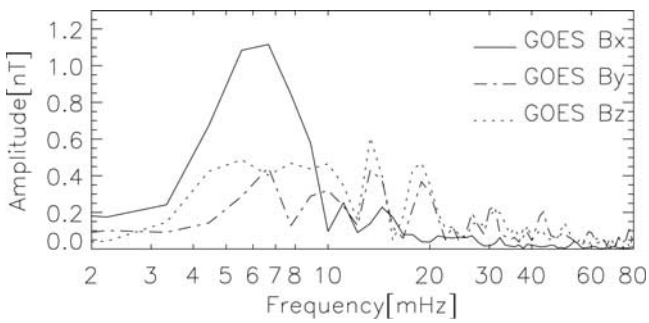

Figure 10. Amplitude spectra of the compressional (B_X; solid line) and transverse (B_Y and B_Z; dash-dotted and dotted lines, respectively) magnetic pulsations at GOES 8.

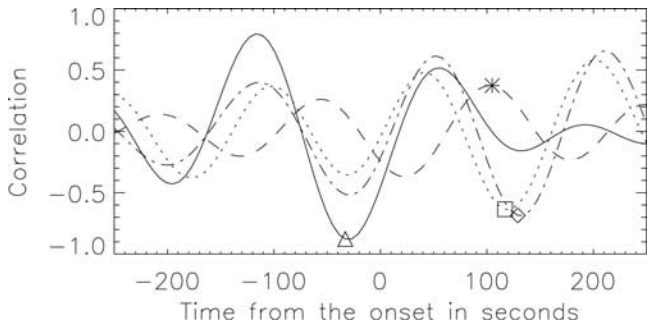

Figure 12. Cross correlations of the signals of Figure 8k (solid line; electric field Z_{GSE} component at Polar), Figure 8c (dashed line; compressional B_X at GOES 8), and Figure 8b (dotted line; magnetic field northward component at NAQ) against the transverse B_Y component at Polar (Figure 8h). Cross correlation of the signal of Figure 8c (compressional B_X at GOES 8) against the magnetic field northward component at NAQ shown in Figure 8b (dash-dotted). The maximum correlations are indicated with triangles, diamonds, squares, and stars. On the basis of the spectral analysis, all of the signals were lowpass filtered (<9 mHz) before the cross correlation.

[27] One of the key observations of this study is the initiation of the pulsations at Polar ~3 min before Polar crossed the plasma boundary indicated by the abrupt electron flux enhancement and diamagnetic effect in the ambient magnetic field. It is relevant to assume that this crossing was related to the plasma sheet expansion and the region confined by the boundary expanded outward. At this boundary, the parallel Poynting flux peaked up to ~0.5 ergs cm^{-2} s^{-1}, which indirectly relates the boundary to considerable auroral activity. The timing of the pulsations and the crossing of the boundary suggests that the plasma sheet activity related to the pulsations was initiated tailward of the boundary. Note also that the Poynting flux observed indicates that the boundary was dynamic rather than static in nature, which suggests that the crossing was not caused, for example by magnetotail flapping.

[28] On the basis of the suggested spatial origin of the pulsations, one may consider the magnetic reconnection of tail lobe flux and the subsequent earthward flows as the ultimate generating mechanism of the observed pulsations. Figure 13 shows a schematic of the key observations. Before the reconnection of tail lobe flux, the reconnection of the plasma sheet field lines must have taken place [*Coroniti*, 1985]. This can be associated with the weak dynamic signature at Polar ~5 min before the oscillations were initiated (recently, *Toivanen et al.* [2001b] identified similar signatures preceding substorm onset signatures at Polar and suggested that such signatures were precursors of the expansion onset, indicating the initiation of the reconnection on plasma sheet field lines prior to lobe field reconnection). In Figure 13a the local thinning of the plasma sheet indicates the location of the reconnection of the plasma sheet field lines that was considered to have started ~5 min before the negative bay onset. Figure 13a also clarifies the notion of the mapping of Polar field line to the distant X-line. This was the case only until the reconnection of the open field lines started, after which the Polar field line mapped closer to the Earth, near the newly formed reconnection site. The fast earthward flows generated by the reconnection of the tail lobe flux have been assumed to be slowed down near the interface of the dipolar and tail-like magnetic field configurations. At this interface, it has been suggested that the cross tail current is diverted through the ionosphere to form the substorm current wedge. This interface is then expected to propagate tailward, and the region of dipolar magnetic field configuration to expand outward. The crossing of the plasma boundary ~3 min after the first onset signatures at Polar can be associated with such an outward expanding region of enhanced fluxes and dipolar field (Figure 13b).

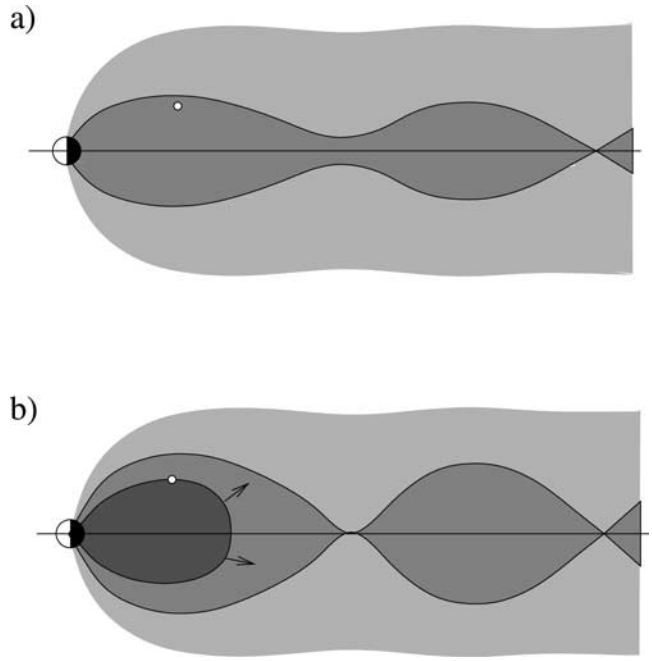

Figure 13. Schematic of Polar's location with respect to the plasma sheet boundary (between the light and medium shadings) and the outward expanding region of high plasma sheet electron fluxes (dark shading). (a) Prior to the onset, Polar was located near the plasma sheet boundary as suggested by the electron and spacecraft data shown in Figure 6. The dent in the plasma sheet indicates the location of the reconnection site of the closed field lines. (b) About 3 min after the onset, Polar was engulfed by the region of enhanced electron fluxes. The pulsations observed originated from the region confined by the NENL and the region of the enhanced electron fluxes.

5. Summary and Discussion

[29] We presented observations from the Polar spacecraft of large-amplitude transverse electromagnetic 6-mHz oscillations in the high-latitude plasma sheet in association with an isolated substorm onset on 19 October 1999. In addition to the Polar observations, we used the Greenland west coast magnetometer chain and the GOES 8 spacecraft. Polar was magnetically conjugate with the Greenland chain, and GOES 8 was located 2 hours west of the chain. The observational geometry was shown in Figure 5. The rich database allowed us to (1) study the spatial origin of the pulsations in the magnetotail, (2) determine the timing of the pulsations relative to negative bay onset and other substorm signatures, and (3) relate the pulsations to the plasma sheet dynamics. The key observations can be listed as the following:

[30] 1. At 0139:00 UT a dynamic signature was observed at Polar including weak variations of electric and magnetic field and associated Poynting flux parallel to the ambient magnetic field. Also the high-energy electron fluxes increased slightly. Importantly, the ambient magnetic field started to decrease at Polar and GOES 8 and decreased continuously until the substorm onset, indicating that the signature was not transient.

[31] 2. At 0144:23 UT the first signatures of the wave activity were observed at Polar. Polar was located near the plasma sheet boundary. 6-mHz oscillations with peak amplitudes of 10 nT and 20 mV m^{-1} were identified. These oscillations were transverse and polarized as $\delta\mathbf{B} \mid Y_{GSM}$ (toroidal). Oscillations with frequencies of 18 mHz or higher were superimposed on the 6-mHz oscillations driving parallel Poynting flux predominantly toward the ionosphere. On the ground, a negative bay with a magnitude of 300 nT was initiated at NAQ. About 2 min later, 6-mHz oscillations with an amplitude of 50 nT was embedded in

the developing auroral electrojet. Also at GOES 8, the magnetic field showed oscillations primarily at frequencies of ~6 mHz (compressional) and 14 mHz (transverse). The 6-mHz oscillations started about two minutes after the timing of the wave activity at Polar. The SAMNET stations west of Greenland at HLL and FAR showed a negative bay and burst of Pi2 pulsations (~17 mHz) starting at about 0146:30 UT. Together with the midlatitude stations of OTT and STJ, SAMNET stations indicated that the center of the substorm current wedge was located near the Greenland west coast chain.

[32] 3. AT 0147:30 UT the outward propagating boundary crosses Polar location. The Poynting flux peaked (~0.5 ergs cm^{-2} s^{-1}) at this boundary indicating strong auroral activity at the Polar foot point. At GOES 8 or on the ground, no dynamic signature was identified.

[33] 4. At 0155 UT the passage of the upward return current of the SCW tailward of GOES 8.

[34] Our interpretation of the key observations is in accordance with the predictions of the NENL model. According to this model, reconnection of the tail lobe magnetic field generates fast earthward flows and the braking of the fast flows in the inner magnetosphere at the interface of the dipolar and tail-like magnetic fields drives field-aligned currents of the substorm current wedge. During the expansion phase the region of dipolar field configuration has been expected to expand tailward [e.g., *Baker et al.*, 1996]. The timing of various signatures was consistent with the prediction of the NENL model. Most notably, the pulsations were first observed near the plasma sheet boundary and later on the ground and at the geostationary orbit. Moreover, the expansion of the region of enhanced electron flux past the Polar location ~3 min after the wave activity started at Polar indicates that the pulsations were initiated before any indication of outward propagating substorm signatures from the inner magnetosphere. Such a timing sequence of the key signatures suggested that the pulsations were initiated between the plasma sheet boundary and the outward propagating boundary of the enhanced plasma sheet electron fluxes and peak Poynting flux. On the basis of these considerations on the spatial origin of the pulsations, we associated the pulsations with the magnetic reconnection, the subsequent Earthward flows, and braking of these flows.

[35] Here, we suggest that under some magnetospheric conditions, the braking of the earthward flow and the diversion of the cross-tail current from the braking region do not occur monotonically. In other words, the process of the flow braking and current diversion may exhibit periodic fluctuations in the strength of the diverted current depending, for example on the ionospheric conditions controlling the closure of the diverted current. Thus it can be suggested the generation mechanism of the observed pulsations could be distinct from the generation mechanisms of the Pi2 pulsations. Note, for example that the frequency of the Pi2s at FAR (17 mHz) were clearly higher than that of the pulsations studied (6 mHz). The oscillations of the flow braking process may have then resulted in compressional waves that were then observed at GOES 8 with the same frequency. The frequency of the waves at GEOS 8 similar to that observed at Polar can be attributed to the behavior of the compression and toroidal waves: the compressional waves such as Pi2s in the inner magnetosphere are known to exhibit a constant frequency over a wide L range, whereas the frequency of toroidal waves varies with L [*Takahashi et al.*, 1996].

[36] Long-period waves are often associated with proposed substorm onset mechanisms in the near-Earth region including those based, for example on the ballooning instability [*Roux et al.*, 1991]. Such association can, however, be biased, because the observations in the near-Earth tail are more frequently acquired near the equator than in the high-latitude plasma sheet. For example, according to statistical results of *Sakurai and McPherron* [1983], magnetic pulsations in the Pi2 frequency range at geostationary distances can be classified primarily by two types of pulsations: (1) a wave with a significant compressional component and (2) a pure transverse wave in the azimuthal component. The oscillations studied here fall into the second category. *Sakurai and McPherron* [1983] concluded that the pure transverse waves are quite rare, while the compressional wave occurs during almost every substorm. In fact, in one of their example events, the toroidal pulsations occurred when the magnetic field was directed almost radially inward (elevation angle of 23°), which is a very tail-like field configuration at the geosynchronous. Under such field conditions the field line of a geostationary spacecraft may map far beyond geostationary distance, as it was the case with Polar during the event studied. Thus the occurrence of the studied pulsations at geostationary spacecraft may roughly correspond to the occurrence of high-energy particle dropouts at such spacecraft.

[37] The results and suggestions presented in this paper are based on a single event. However, on the basis of the event studied, we were able to argue that the in situ observations of magnetic pulsations in the frequency range of Pi2 and Pc5 pulsations obtained in the high-latitude plasma sheet are an important extension to the data sets acquired in the equatorial plasma sheet and lead to new insights into the physics of the magnetospheric substorms.

[38] **Acknowledgments.** This work was supported by grants from the NASA/GGS program. The work of W. K. Peterson was supported by NASA grant NAG5-11351. H. J. Singer appreciates support from NOAA. The work at UCLA was supported by NASA under research grant NAG5-11324. The results of the HYDRA investigation were made possible by the decade-long hardware efforts of groups led at NASA GSFC by K. Ogilvie, at UNH by R. Torbert, at MPAe by A. Korth, and UCSD by W. Fillius. We also want to thank D. K. Milling for the SAMNET data. The midlatitude magnetosmeter data from OTT and STJ were supplied by the Geological Survey of Natural Resources Canada.

[39] Lou-Chuang Lee thanks Akira Kadokura and Naiguo Lin for their assistance in evaluating this paper.

References

Baker, D. N., T. I. Pulkkinen, V. Angelopoulos, W. Baumjohann, and R. L. McPherron, Neutral line model of substorms: Past results and present view, *J. Geophys. Res.*, *101*, 12,975–13,010, 1996.

Blake, J. B., et al., Comprehensive energetic particle and pitch angle distribution experiment on Polar (CEPPAD), *Space Sci. Rev.*, *71*, 531–562, 1995.

Coroniti, F. V., Explosive tail reconnection: The growth and expansion phase of the magnetospheric substorms, *J. Geophys. Res.*, *90*, 7427–7447, 1985.

Cramoysan, M., R. Bunting, and D. Orr, The use of a model current wedge in the determination of the position of substorm current systems, *Ann. Geophys.*, *13*, 583–594, 1995.

Erickson, G. M., N. C. Maynard, W. J. Burke, G. R. Wilson, and M. A. Heinemann, Electromagnetics of substorm onsets in the near-geosynchronous plasma sheet, *J. Geophys. Res.*, *105*, 25,265–25,290, 2000.

Harvey, P., et al., The electric field instrument on the Polar satellite, *Space Sci. Rev.*, *71*, 583–596, 1995.

Keiling, A., J. R. Wygant, C. Cattell, M. Johnson, M. Temerin, F. S. Mozer, C. A. Kletzing, J. Scudder, and C. T. Russell, Large Alfvén wave power in the plasma sheet boundary layer during the expansion phase of substorms, *Geophys. Res. Lett.*, *27*, 3169–3172, 2000.

Lui, A. T. Y., Current disruption in the Earth's magnetosphere: Observations and models, *J. Geophys. Res.*, *101*, 13,067–13,088, 1996.

McPherron, R. L., C. T. Russell, and M. P. Aubry, Satellite studies of magnetospheric substorms on August 15, 1968, Phenomenological model for substorms, *J. Geophys. Res.*, *78*, 3131–3149, 1973.

Olson, J. V., Pi2 pulsations and substorm onsets: A review, *J. Geophys. Res.*, *104*, 17,499–17,520, 1999.

Pulkkinen, T. I., et al., Modeling the growth phase of a substorm using the Tsyganenko model and multispacecraft observations: CDAW-9, *Geophys. Res. Lett.*, *18*, 1963–1966, 1991.

Roux, A., S. Perraut, P. Robert, A. Morane, A. Pedersen, A. Korth, G. Kremser, B. Aparacio, D. Rodgers, and R. Pellinen, Plasma sheet instabillity related to the westward traveling surge, *J. Geophys. Res.*, *96*, 17,697–17,714, 1991.

Russell, C. T., R. C. Snare, J. D. Means, D. Pierce, D. Dearborn, M. Larson, G. Barr, and G. Le, The GGS/Polar magnetic fields investigation, *Space Sci. Rev.*, *71*, 563–582, 1995.

Sakurai, T., and R. L. McPherron, Satellite observations of Pi2 activity at synchronous orbit, *J. Geophys. Res.*, *88*, 7015–7027, 1983.

Scudder, J., et al., RA-A 3-dimensional electron and ion hot plasma instrument for the Polar spacecraft of the GGS mission, *Space Sci. Rev.*, *71*, 459–495, 1995.

Southwood, D. J., and W. F. Stuart, Pulsations at the substorm onset, in *Dynamics of the Magnetosphere*, edited by S.-I. Akasofu, pp. 341–355, D. Reidel, Norwell, Mass., 1980.

Takahashi, K., B. J. Anderson, and S.-I. Ohtani, Multisatellite study of nightside transient toroidal waves, *J. Geophys. Res.*, *101*, 24,815–24,825, 1996.

Toivanen, P. K., et al., Reconciliation of the substorm onset determined on the ground and at the Polar spacecraft, *Geophys. Res. Lett.*, *28*, 107–110, 2001a.

Toivanen, P. K., D. N. Baker, W. K. Peterson, X. Li, E. F. Donovan, A. Viljanen, A. Keiling, J. R. Wygant, and C. A. Kletzing, Plasma sheet dynamics observed by the Polar spacecraft in association with substorm onsets, *J. Geophys. Res.*, *106*, 19,117–19,130, 2001b.

Tsyganenko, N. A., A magnetospheric magnetic field model with a warped tail current sheet, *Planet. Space Sci.*, *37*, 5–20, 1989.

Wygant, J. R., et al., Polar spacecraft based comparisons of intense electric fields and Poynting flux near and within the plasma sheet-tail lobe boundary to UVI images: An energy source for the Aurora, *J. Geophys. Res.*, *105*, 18,675–18,692, 2000.

D. N. Baker and W. K. Peterson, Laboratory for Atmospheric and Space Physics, University of Colorado, Boulder, CO 80309-0590, USA.

C. A. Kletzing, Department of Physics and Astronomy, University of Iowa, Iowa City, IA 52242, USA.

C. T. Russell, Institute of Geophysics and Planetary Physics, University of California at Los Angeles, Los Angeles, CA 90095-1567, USA.

H. J. Singer, Space Environment Center, NOAA, 325 Broadway, Boulder, CO 80303, USA.

P. K. Toivanen, Geophysical Research, Finnish Meteorological Institute, P.O. Box 503, FIN-00101, Helsinki, Finland. (petri.toivanen@fmi.fi)

J. Watermann, Danish Meteorological Institute, Lyngbyvej 100, DK-2100 Copenhagen, Denmark.

J. R. Wygant, School of Physics and Astronomy, University of Minnesota, Minneapolis, MN 55455, USA.

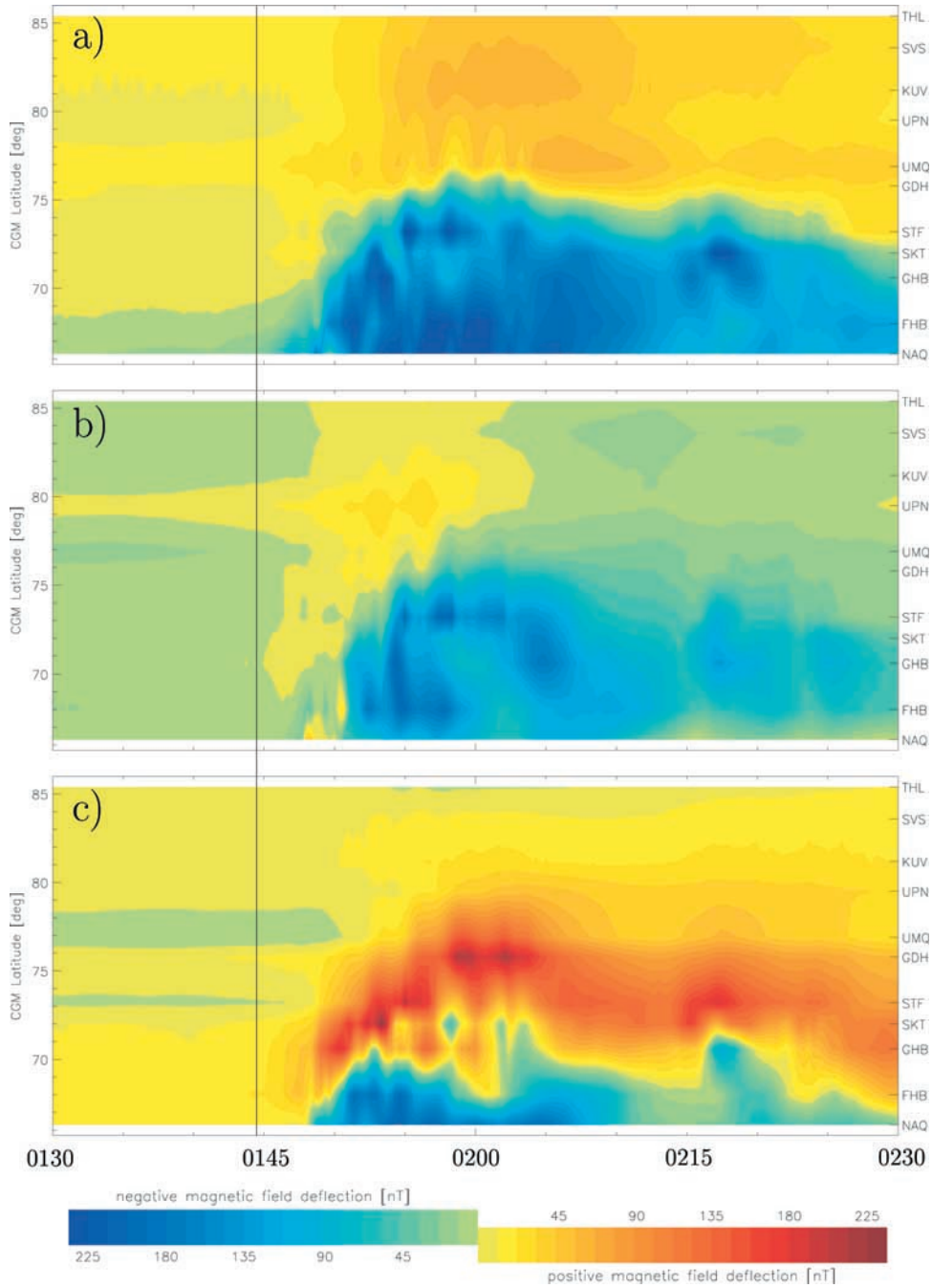

Figure 1. Deflections of the horizontal (a) north-south and (b) east-west, and (c) vertical magnetic field CGM components as functions of CGM latitude and time (CGM, Corrected Geomagnetic). The magnitudes were interpolated in the latitude range of the Greenland west coast stations. At 0144:23 (vertical line), Polar observed the first dynamical signatures (defined in Figure 8k) associated with the ground onset.

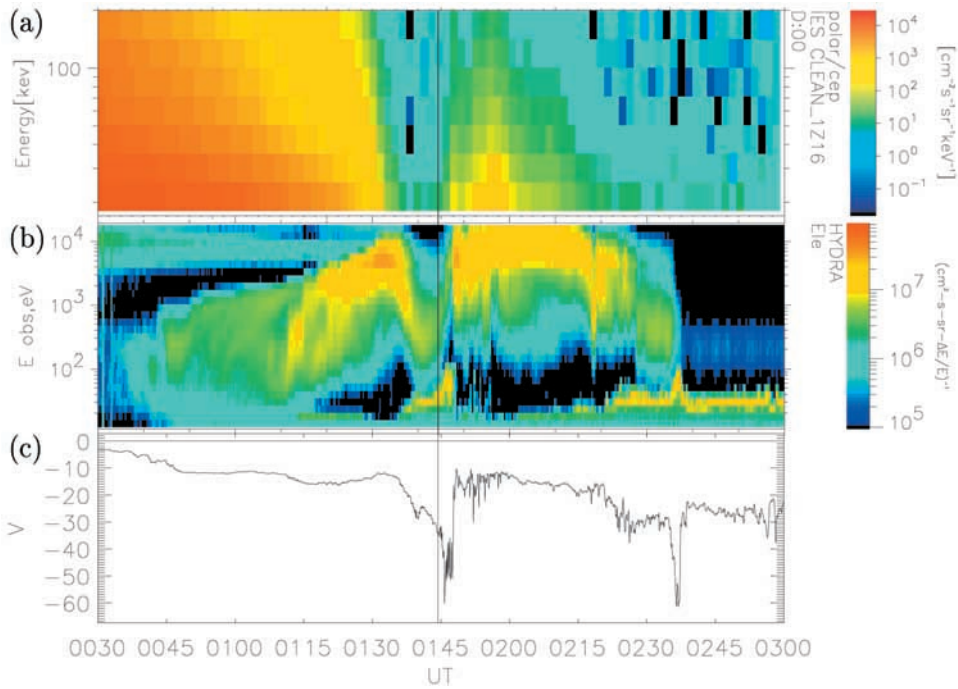

Figure 6. Overview of (a) high-energy electrons (17–200 keV), (b) plasma sheet electrons (0.1–20 keV), and (c) spacecraft potential as observed by CEPPAD/IES, HYDRA, and EFI, respectively.

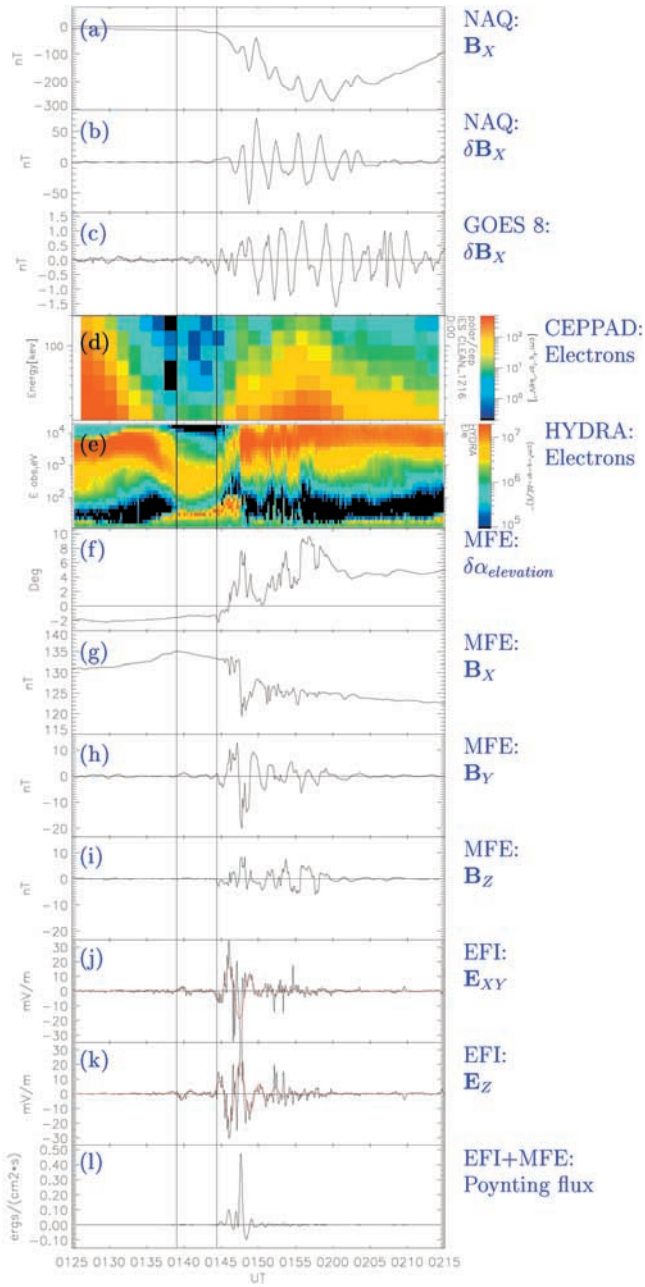

Figure 8. (a) The northward component at NAQ, (b) the 180-s detrended northward component at NAQ, (c) the 180-s detrended ambient field at GOES 8, (d) CEPPAD electrons (17–200 keV), (e) HYDRA electrons (0.1–20 keV), (f) measured magnetic field elevation angle with respect to the elevation angle of the T89 model, (g) ambient magnetic field at Polar, (h) Y and (i) Z components of the perpendicular magnetic field at Polar, (j) XY_{GSE} and (k) Z_{GSE} components at Polar (the red curves show the low-pass filtered (<7 mHz) 180-s detrended signals), and (l) Parallel Poynting flux (positive toward the ionosphere). The vertical lines indicate the onset time (0144:23 UT) and the transient signature at 0139:00 UT as determined from the EFI instrument (Figure 8k).